MODELING OF ULTRA-COLD AND CRYSTALLINE ION BEAMS*

H. Okamoto#, H. Sugimoto, Hiroshima University, Hiroshima, Japan
Y. Yuri, Takasaki Advanced Radiation Research Institute, JAEA, Gumma, Japan
M. Ikegami, Keihanna Research Laboratory, Shimadzu Corporation, Kyoto, Japan
J. Wei, Tsinghua University, Beijing, China

Abstract

An ultimate goal in accelerator physics is to produce a "zero-emittance" beam, which is equivalent to making the beam temperature the absolute zero in the center-of-mass frame. At this limit, if somehow reached, the beam is Coulomb crystallized. Schiffer and co-workers first applied the molecular dynamics (MD) technique to study the fundamental features of various Coulomb crystals. Their pioneering work was later generalized by Wei et al. who explicitly incorporated discrete alternating-gradient (AG) lattice structures into MD simulations. This paper summarizes recent numerical efforts made to clarify the dynamic behavior of ultra-cold and crystalline ion beams. The MD modeling of beam crystallization in a storage ring is reviewed, including how one can approach the ultra-low emittance limit. Several possible methods are described of cooling an ion beam three-dimensionally with radiation pressure (the Doppler laser cooling).

INTRODUCTION

Mutual Coulomb interactions among stored particles play a substantial role in beam dynamics especially when those particles are densely distributed in phase space [1,2]. The volume occupied by the particles in six-dimensional phase space is called "emittance" that can directly be linked to the beam "temperature" measured in the center-of-mass frame. In theory, the emittance of a beam converges to zero (except for quantum noises) at the ultra-low temperature limit [3]. It can thus be said that space-charge-induced phenomena become more prominent as the emittance or temperature goes down.

The emittance is approximately conserved if the rate of Coulomb collisions between individual particles is low [4]. That is basically due to the Hamiltonian nature of lattice elements (magnets, cavities, etc.) that only produce conservative forces. In practice, however, we almost always prefer a beam with a lower emittance. To meet this general requirement, we must introduce dissipative interactions into the system to "cool" the beam. Needless to say, the ultimate goal of cooling is to make the beam temperature the absolute zero.

Many questions arise, however: is it really possible in principle to establish a zero-emittance state? Can such an ultimate state, if it exists, be stable? How does the beam look like at that limit? These questions have been answered since the mid 1980's [5-13]. Schiffer and co-workers first carried out systematic theoretical researches on strongly-coupled non-neutral plasmas by employing the MD technique [5-9], but their work was based on the smooth approximation that may eliminate possible realistic effects in cooler storage rings. This fact motivated the later, more sophisticated MD work by Wei et al. who took discrete lattice structures into account [10-13]. Their MD simulations actually revealed essential differences between ultra-cold states in a uniform channel and those in an AG channel. Through all these continuous efforts, it is now strongly believed that stable zero-emittance beams can exist, at least, in theory.

The purpose of this paper is to give a brief review of computer modelling of ion beams in the ultra-low temperature regime. After showing the primary conditions to form and maintain a crystalline ion beam in a storage ring, we outline the MD method employed generally for crystalline-beam studies. We then proceed to the description of several cooling models including the Doppler laser cooling [14,15] that is currently the only solution toward beam crystallization. Although the Doppler limit is actually very close to the absolute zero, the powerful laser cooling force only operates in the longitudinal direction of beam motion [16,17]. It is thus necessary to somehow make it work three-dimensionally. For this purpose, we here consider the *resonant coupling method* (RCM) that can easily be implemented in a real storage ring [18,19]. Finally, a unique storage-ring lattice free from momentum dispersion [20,21] is described which can resolve the problem of "tapered cooling" [12,22].

CRYSTALLINE BEAMS

Schiffer, Hasse and others numerically demonstrated that a system of many identical charged particles confined by a time-independent harmonic potential exhibits a spatially ordered configuration at the low-temperature limit [5-9]. This phenomenon is referred to as "Coulomb crystallization". In this unique state of matter, the Coulomb repulsion among particles just balances with the external focusing potential. Suppose a coasting ion beam, for instance. If the line density is sufficiently low, all ions are aligned along the design beam orbit at equal intervals (string crystal). By increasing the line density, we can convert this one-dimensional (1D) configuration into a two-dimensional (2D) (zigzag crystal). The zigzag crystal is eventually transformed to a three-dimensional (3D) figure (shell crystal) if we put more ions in the beam. The threshold line density from a particular crystalline structure to another can be estimated from the Hasse-Schiffer theory [8]. Similar structural transitions occur even for bunched beams. Figure 1 shows a typical multi-shell Coulomb crystal predicted by a MD simulation.

*Work supported in part by Grants-in-Aid for Scientific Research.
#okamoto@sci.hiroshima-u.ac.jp

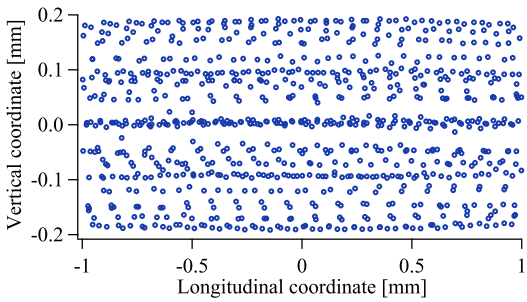

Figure 1: Side view of a typical 3D Coulomb crystal numerically obtained with a MD simulation code.

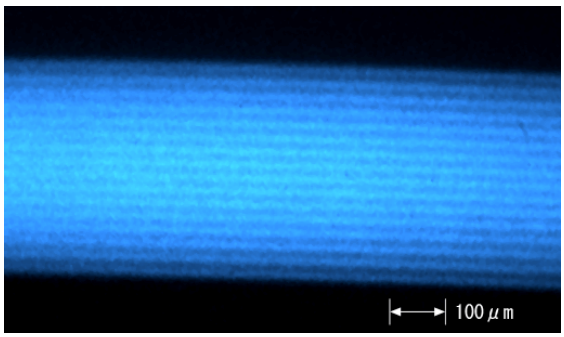

Figure 2: Laser-induced fluorescence from a multi-shell Coulomb crystal formed in a linear Paul trap at Hiroshima University.

When the external force is uniform and time-independent as assumed in early papers on Coulomb crystals [5-9], each particle is frozen at a certain fixed point in the rest frame once the beam reaches a crystalline ground state. The situation is definitely different in a storage ring where the beam experiences periodic driving forces all the time. The periodic change of the focusing potential excites resonant instability under a specific condition satisfied. It is particularly important to avoid crossing *linear* (second order) resonance stopbands throughout a cooling process toward the absolute zero. To eliminate the possibility of dangerous resonance crossing, the bare betatron phase advance per lattice period must be less than 90 degrees [12,23]:

$$\nu_{x(y)} < N_{sp}/4, \qquad (1)$$

where (ν_x, ν_y) are the horizontal and vertical betatron tunes, and N_{sp} denotes the lattice superperiodicity of the ring. The time-dependency of the external potential also enhances heating from *intrabeam scattering* [24,25]; we thus need to provide sufficiently strong transverse cooling force to overcome this effect. Another primary condition pointed out by Wei et al. is the following:

$$\gamma < \gamma_T, \qquad (2)$$

which means that the beam energy γ (the Lorentz factor) must be below the transition energy γ_T of the ring.

Various Coulomb crystals have now been realized *experimentally* in ion traps [26-28]. It is actually straightforward to produce an ultra-cold ion plasma in a trap by using the Doppler cooling technique. Figure 2 is a laser-induced fluorescence image of a $^{40}Ca^{+}$ plasma laser-cooled in a linear Paul trap. There is no doubt that a multi-shell crystalline structure has been formed. It is indeed possible to make string and zigzag crystals as well. This experimental evidence probably convinces many people that it must be possible to crystallize an ion beam in a similar way. In reality, however, nobody has succeeded in producing a crystalline beam in spite of serious attempts by European groups [16,17,29,30]. Although "moving" Coulomb crystals were generated in a ring-shaped Paul trap system [31,32], crystalline beams in a real storage-ring accelerator have the nature more complex than Coulomb crystals in such a compact low-energy device. In addition, the lattice parameters are not so flexible which often prevents us from approaching an ultra-low temperature state [33]. How to achieve efficient 3D laser cooling in a storage ring is also a big issue.

MD APPROACH

Periodic Boundary Condition

The Particle-In-Cell (PIC) algorithm has often been adopted to study the dynamic behavior of space-charge-dominated beams. Beam crystallization is, however, clearly beyond the scope of the PIC method that relies on spatial meshes and macro-particles. Since collective interactions over the whole beam and Coulomb collisions among individual particles both play an important role at low temperature, we have to compute the space-charge potential as precisely as possible. The best way is to simply sum up the Coulomb potentials of all particles, but that is indeed impractical even with a modern high-performance computer when the beam consists of a large number of particles.

In MD simulations, the so-called periodic boundary condition is employed to save computing time. We first slice the beam in the longitudinal direction and load some number of "real" particles (not "macro" particles) in the reference cell we are looking at. Within this particular cell, interparticle Coulomb interactions are calculated from the potential of the form

$$\phi_{short}^{(j)} = \frac{1}{\sqrt{(x-x_j)^2 + (y-y_j)^2 + (z-z_j)^2}}, \qquad (3)$$

where (x, y, z) is the spatial coordinates of a particle, and (x_j, y_j, z_j) the coordinates of one of the other particles. When the cell contains n particles, the short-range Coulomb forces acting upon the particle at (x, y, z) are evaluated by summing up Eq. (3) over all $n-1$ partners.

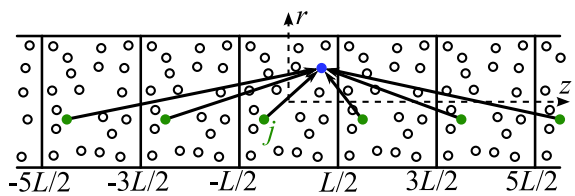

Figure 3: Periodic boundary condition

If n is not too large, the CPU time required for this process should be reasonable. Now, the question is how to compute the long-range Coulomb forces coming from other cells. The MD algorithm assumes that all longitudinal cells have an identical particle distribution at each integration step, as illustrated in Fig. 3. Then, the long-range Coulomb potential generated by the jth particle's images in all cells can be reduced to the Ewald-type integral [34]:

$$\phi_{long}^{(j)} = \frac{2}{L}\int_0^\infty \frac{\cosh(kz^{(j)}/L)J_0(kr^{(j)}/L)-1}{e^k-1}dk, \quad (4)$$

where L is the cell length, J_0 is the Bessel function of zero-th order, $z^{(j)} = |z - z_j|$ $(-L/2 < z^{(j)} < L/2)$, and $r^{(j)} = \sqrt{(x-x_j)^2 + (y-y_j)^2}$. Although the beam is not perfectly uniform in the longitudinal direction, this should be a good approximation because the total long-range potential is probably insensitive to the details of the image charge distribution. The cell length L should be neither too short nor too long, so that we have a proper number of real particles in the reference cell. It has been confirmed that, as long as the ratio n/L is fixed, we always reach the same crystalline structure.

Beam-Frame Hamiltonian

In order to apply the periodic boundary condition, we have to observe the beam motion in the center-of-mass frame. Strictly speaking, the general relativity formalism is required to derive the correct equations of motion because the beam is not in an inertial system. Let us here suppose an ion beam travelling at the speed βc with c being the light velocity. For simplicity, consider only dipole and quadrupole magnetic fields. Then, the beam-frame Hamiltonian is approximately given by [35]

$$H = \frac{p_x^2 + p_y^2 + p_z^2}{2} - \frac{\gamma}{\rho}xp_z + \frac{x^2}{2\rho^2} - \frac{K(s)}{2}\left(x^2 - y^2\right) + \frac{r_p}{\beta^2\gamma^2}\phi, \quad (5)$$

where the scaled canonical variables are $(x, y, z; p_x, p_y, p_z)$, ρ is the local curvature of the design beam orbit, $K(s)$ corresponds to the focusing gradients of quadrupole magnets, r_p is the classical radius of the particle, and the independent variable is the path length $s = \beta\gamma c \cdot t$ with t being proper time. The scalar Coulomb potential is calculated in a MD code from $\phi = \sum_j (\phi_{short}^{(j)} + \phi_{long}^{(j)})$. Not surprisingly, H has the form identical to the well-known Hamiltonian for standard beam-orbit theories. We have developed a MD code "CRYSTAL" that integrates this Hamiltonian motion in a symplectic manner. Solenoid magnets, radio-frequency (rf) cavities, and other insertion elements can also be incorporated in the code, if necessary.

When the beam is bunched, the CRYSTAL code automatically set the MD cell length equal to the rf bucket size, assuming that all bunches have an identical particle distribution. We have confirmed that, at low temperature, the Coulomb potentials from other bunches are generally quite weak.

COOLING MODELS

Cooling interactions must be introduced separately from the Hamiltonian framework because they are not conservative. Several cooling models can be considered in the CRYSATL code to study the dynamics of cold beams.

Linear Friction

The simplest cooling force is the linear 1D friction defined by

$$\Delta p_q = -f_q p_q^{in} \quad (q = x, y, z), \quad (6)$$

where f_q is the constant friction coefficient, and Δp_q stands for the momentum change in q-direction before and after the cooling section; namely, $\Delta p_q = p_q^{out} - p_q^{in}$. This cooling force just tries to equalize the velocities of all particles. The linear friction can certainly cool regular *hot* beams, but at very low temperature, it works as a heating source. For example, unlike in a uniform focusing channel, the betatron oscillations of particles never vanish in an AG lattice as long as the beam has finite transverse extent.

Tapered Cooling

As mentioned above, too strong a transverse linear friction eventually starts to heat up the beam due to the oscillatory nature of the stationary state. The same argument also applies to the longitudinal motion because of the existence of dipole fields in a storage ring. Once a crystalline ground state is reached, particles with different horizontal positions follow slightly different closed orbit every turn. On the other hand, their revolution frequencies must be identical to maintain the ordered structure. This means that the average longitudinal speeds of those particles are different depending on the horizontal coordinates. Therefore, the linear friction as in Eq. (6) again operates as a heating source in the longitudinal direction. To compensate the *dispersive* heating at ultra-low temperature, the *tapered* cooling force is necessary [12,22]:

$$\Delta p_z = -f_z(p_z^{in} - C_{xz}x^{in}), \quad (7)$$

where C_{xz} is the tapering factor that depends on the lattice design [36]. The tapered force yields not only longitudinal but also horizontal cooling effects when it is applied to the beam at a position with finite momentum dispersion [22].

Laser Cooling

The longitudinal dissipative force $F_{+(-)}$ generated by a laser light co-propagating (counter-propagating) with an ion beam can be expressed as [14,15]

$$F_\pm = \pm\frac{1}{2}\hbar k_L \Gamma \frac{S_L}{1 + S_L + (2\delta_\pm/\Gamma)^2}, \quad (8)$$

where Γ is the natural linewidth of the cooling transition, k_L is the wave number of the laser, S_L is the saturation parameter, and $\delta_{+(-)}$ is the detuning of the co-propagating (counter-propagating) laser frequency from the natural resonant frequency ω_0 of the ion. When the co-propagating (counter-propagating) laser frequency in the laboratory frame is $\omega_{+(-)}$, we have the Doppler-shifted detuning $\delta_\pm \approx \omega_\pm \gamma[1 \mp \beta(1 + p_z/\gamma)] - \omega_0$. Assuming a Gaussian laser, the saturation parameter is given by $S_L = S_0 \exp[-2(x^2 + y^2)/w^2]$, where S_0 corresponds to the peak saturation parameter on the axis of laser propagation, and w is the laser spot size that depends on the Rayleigh length z_R. When the center of a laser cooling section is located at the longitudinal coordinate s_0, we can write $w(s) = w_0\sqrt{1 + \gamma^2(s - s_0)^2/z_R^2}$ with w_0 being the waist size of the laser.

The Doppler limit T_D of laser cooling is determined by the balance between the dissipative force in Eq. (8) and diffusive heating originating from the random nature of photon emission and absorption. In the simple 1D case, T_D can be evaluated from the formula $k_B T_D/2 = \hbar\Gamma/4$, where k_B is the Boltzmann constant. In the CRYSTAL code, a proper amount of random kick is applied to the beam in every integration step to include the diffusive heating effect. To check the reliability of our laser-cooling algorithm, we performed test simulations changing some fundamental parameters. An example is shown in Fig. 4 where the final equilibrium temperature reached in our laser-cooling simulation is plotted as a function of integration time step. The horizontal straight line corresponds to the theoretical Doppler limit that agrees fairly well with the CRYSTAL simulation results unless the integration step is too large.

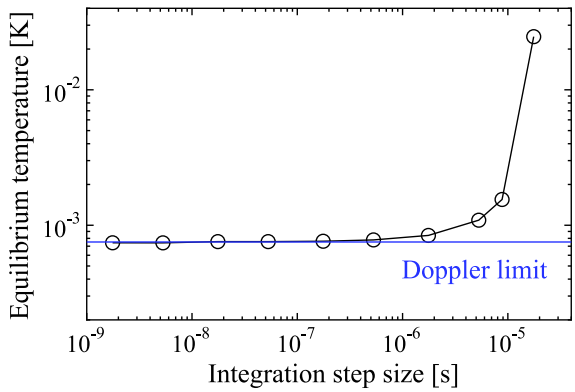

Figure 4: Results of Monte-Carlo simulations to test the laser-cooling model. Low-energy $^{24}Mg^+$ ions have been assumed in this example.

RESONANT COUPLING SCHEME

Principle

In order for the Doppler cooling mechanism to be effective, each ion must absorb many photons while it passes through a cooling section. This requirement can readily be met in the longitudinal direction by introducing the laser light along the beam orbit in a straight section. As to the transverse directions, it is practically impossible to achieve efficient, direct laser cooling because we cannot ensure a large overlap between the beam and laser. Unlike an ion plasma in a compact trap, a typical ion beam in a storage ring is much hotter and thinner, which makes it extremely difficult to accomplish 3D laser cooling.

A possible solution to extend the powerful longitudinal laser-cooling force to the transverse dimensions is the use of dynamic coupling that correlates one dimension to the others [18]. Mathematically, what we must do is to create additional linear potentials proportional to $x \cdot z$ and $y \cdot z$ (or $x \cdot y$). We then move the operating point of the storage ring to excite linear coupling resonances:

$$\nu_x - \nu_y \approx \text{integer}, \quad \nu_x - \nu_z \approx \text{integer}, \tag{9}$$

where ν_z is the synchrotron tune. As theoretically demonstrated in previous papers [18,19], the transverse indirect cooling rate is considerably enhanced under these conditions. The effectiveness of RCM has been partially confirmed in a storage-ring experiment [37] where the method was actually employed to improve the vertical cooling efficiency. In this experiment, a solenoid magnet was turned on to produce the linear $x \cdot y$ coupling.

Coupling Sources

There are several practical ways to provide the linear coupling potential required for indirect transverse cooling. The excitation of horizontal-vertical coupling is particularly easy; we simply put either a skew quadrupole magnet or a solenoid. It is also straightforward to couple the longitudinal motion of a stored particle with the horizontal motion; all we have to do is to place a regular rf cavity at a dispersive position [19]. An alternative solution for longitudinal-transverse coupling is the use of coupling rf cavities operating in a deflective mode [18]. The coupling-cavity scheme is more flexible in controlling the transverse cooling efficiency because it does not rely on the dispersion function of the lattice.

Another interesting option for indirect transverse cooling is the Wien filter [38]. The single-particle motion within this static electromagnetic device approximately obeys the Hamiltonian

$$H_W = \frac{p_x^2 + p_y^2 + p_z^2}{2} + \frac{1}{2}\kappa_x^2 x^2 - \kappa_x x p_z, \tag{10}$$

where κ_x is a constant parameter proportional to the filter voltage. As pointed out in Ref. [38], a sort of tapered force defined by Eq. (7) is naturally developed when we apply a cooling laser to stored ions within the filter. The momentum dispersion must, therefore, be finite in the straight section where this device is located. It is worthy to recall that tapered cooling requires no synchro-betatron resonance to enhance the horizontal cooling rate [22]. We

can thus strongly cool even coasting beams. Efficient vertical cooling can very easily be carried out with RCM by equalizing two betatron tunes (ν_x, ν_y) and then switching on either a solenoid or a skew quadrupole.

MD RESULTS

It has been demonstrated in many previous papers that beam crystallization is theoretically feasible under several conditions satisfied. The necessary conditions include not only Eqs. (1) and (2) but also efficient transverse cooling plus tapering. In practice, however, it is difficult to meet all these requirements simultaneously. For example, the condition (1) cannot strictly be fulfilled unless we execute beam cooling in all lattice periods. If we bunch the beam with a single rf cavity, that also weakly breaks the lattice symmetry, reducing N_{sp} to unity. The bare betatron tune $\nu_{x(y)}$ then has to be less than 0.25 per turn, which is clearly unacceptable in a regular storage ring.

We have performed a number of systematic MD simulations to see how close we can come to a crystalline state with existing technologies. First of all, laser cooling has to be chosen for our final goal because of its ultra-low limiting temperature. Although several other cooling methods are available, none of them can reach the temperature range close to the absolute zero. Then, we need to enhance the transverse cooling rate in some way. The best option for this purpose should be the application of RCM, considering its simplicity; in fact, all we need is to adjust the betatron tunes to proper resonant values if linear coupling sources are present in the ring. Figure 5 shows a MD result in which we have assumed low-energy $^{24}Mg^{+}$ ions circulating in the cooler storage ring "S-LSR" at Kyoto University [21]. Clearly, a coasting string crystal has been formed. In this example, a *horizontal* Wien filter is used to activate linear synchro-betatron coupling, while a weak solenoid field is switched on for $x \cdot y$ coupling. S-LSR actually has a solenoid magnet (originally for electron cooling) in one of six straight sections. The bare tunes have been set at $(\nu_x, \nu_y) = (1.46, 1.46)$ to improve the vertical cooling rate with RCM. The ordered configuration in Fig. 5, whose normalized root-mean-squared (rms) emittance is below 10^{-12} m·rad, lasts many turns even without the cooling force. It is also possible to form a zigzag crystalline beam while its stability is not guaranteed. Note that, by switching on an rf cavity, we can establish string and zigzag-like configurations of finite lengths (bunched crystals). In that case, the Wien filter is no longer necessary because, as explained in the last section, a regular rf cavity sitting in a dispersive position naturally induces synchro-betatron coupling.

In contrast to 1D and 2D crystals, none of numerical attempts to produce a stable shell crystal with realistic methods have been successful. There are two primary obstacles that prevent the formation of stable 3D crystalline structures:

- Transverse collective instability (linear coherent resonance) due to the lattice symmetry breakdown originating from local cooling forces and coupling sources.
- Lack of an optimal tapered force.

We immediately recognize that it is not easy to evade the first obstacle in practice. The second one is also quite troublesome. Although a Wien filter provides a tapered force, it is difficult to adjust the tapering coefficient to the optimum value [38]. Even if the optimum tapering is realized somehow, the filters have to be placed in all superperiods to keep the high lattice symmetry, which is not realistic in general.

DISPERSION-FREE LATTICE

One of the two obstacles mentioned above (i.e. lack of an optimal tapered force) can be overcome by introducing special bending elements [20]. Since the necessity of the tapered force comes from the existence of momentum dispersion in a usual storage ring, what we should try is to minimize dispersive effects. It is actually possible to eliminate linear dispersion all around the storage ring by combining an electro-static dipole field with a magnetic dipole [20].

The dispersion-free bending element enables us to construct multi-shell crystalline structures, as depicted in Fig. 6, without the use of the tapered force. The bunched

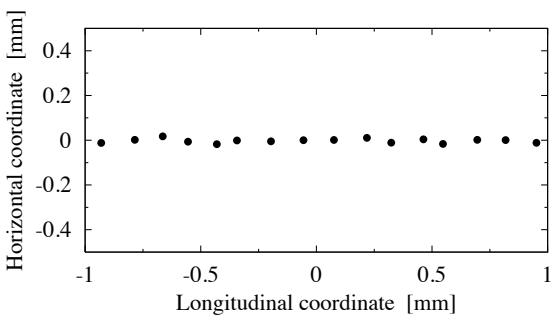

Figure 5: Spatial configuration of an ultra-cold ion beam predicted by a MD simulation in which the realistic laser-cooling model and the lattice of S-LSR have been considered.

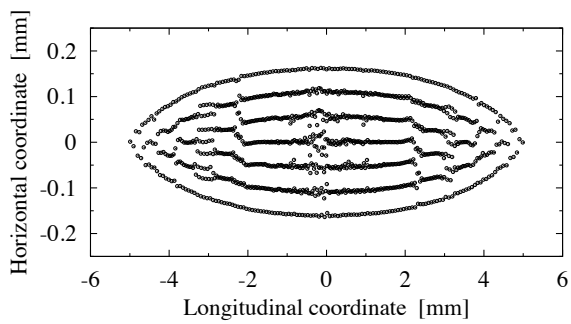

Figure 6: Ordered structure formed in a ten-fold symmetric test storage ring operating in a dispersion-free mode. The linear friction model in Eq. (6) has been employed to cool a bunched $^{24}Mg^{+}$ beam.

3D crystalline state was actually reached with the linear friction model in Eq. (6). The ordered beam in Fig. 6 is, however, unstable without the cooling force; the crystalline structure is destroyed as soon as we stop cooling the beam. This is because in the present simulation, we put only one rf cavity in the test ring to bunch the beam. If rf cavities are placed and excited in all lattice periods, then the stability of the crystalline beam is remarkably improved. In any case, it is impossible to form such an ordered 3D configuration as shown in Fig. 6 unless the ring is operated in the dispersion-free mode.

CONCLUSIONS

We have surveyed relatively recent MD results on Coulomb crystallization of ion beams circulating in a storage ring. Emphasis is placed upon the importance of including the actual lattice structure of the ring into MD simulations. In fact, the periodic nature of AG focusing and momentum dispersion peculiar to a circular machine make the dynamic behavior of crystalline beams much more complex than that of Coulomb crystals in a harmonic potential. To form various crystalline beams, we need a storage ring that has a high superperiodicity and is equipped with a laser cooler. It is particularly important to preserve the lattice symmetry as strictly as possible, so that the destructive effect from transverse coherent instability is minimized. In a regular ring, it is also strongly required to develop an optimal tapered force in order to avoid dispersive heating at ultra-low temperature.

MD simulations indicate that 1D and 2D crystalline beams can be generated with advanced beam cooling techniques, e.g. 3D laser cooling based on RCM. The use of the dispersion-free bending element may enable us to form even 3D crystalline structures (while it depends on how well we can maintain the lattice symmetry). In any case, a careful combination of state-of-the-art accelerator technologies will make it possible to produce an ultra-cold beam that has a normalized rms emittance of the order of 10^{-10} m·rad or even lower.

REFERENCES

[1] M. Reiser, Theory and Design of Charged Particle Beams (Wiley, New York, 1994).

[2] T. Katayama and T. Koseki (eds.), Proc. of Int. Workshop on *Beam Cooling and Related Topics* (COOL 03) (Yamanashi, Japan, 2003).

[3] H. Okamoto, H. Sugimoto, and Y. Yuri, to be published in J. Plasma Fusion Res.

[4] This is not the case for high-energy electron and positron beams that naturally radiate photons.

[5] J. P. Schiffer and P. Kienle, Z. Phys. A **321**, 181 (1985).

[6] A. Rahman and J. P. Schiffer, Phys. Rev. Lett. **57**, 1133 (1986).

[7] J. P. Schiffer, Phys. Rev. Lett. **61**, 1843 (1988).

[8] R. W. Hasse and J. P. Schiffer, Ann. Phys. (N.Y.) **203**, 419 (1990).

[9] R. W. Hasse and V. V. Avilov, Phys. Rev. A **44**, 4506 (1991).

[10] J. Wei, X.-P. Li, and A. M. Sessler, Phys. Rev. Lett. **73**, 3089 (1994).

[11] J. Wei, X.-P. Li, and A. M. Sessler, "Crystalline Beams", AIP Conf. Proc. **335**, p.224 (1995).

[12] J. Wei, H. Okamoto, and A. M. Sessler, Phys. Rev. Lett. **80**, 2606 (1998).

[13] Y. Yuri and H. Okamoto, Phys. Rev. ST Accel. Beams **8**, 114201 (2005).

[14] T. Hänsch and A. Schawlow, Opt. Commun. **13**, 68 (1975).

[15] D. J. Wineland and H. Dehmelt, Bull. Am. Phys. Soc. **20**, 637 (1975).

[16] S. Schröder et al., Phys. Rev. Lett. **64**, 2901 (1990).

[17] J. S. Hangst et al., Phys. Rev. Lett. **67**, 1238 (1991).

[18] H. Okamoto, A. M. Sessler, and D. Möhl, Phys. Rev. Lett. **72**, 3977 (1994).

[19] H. Okamoto, Phys. Rev. E **50**, 4982 (1994).

[20] M. Ikegami et al., Phys. Rev. ST Accel. Beams **7**, 120101 (2004).

[21] A. Noda, M. Ikegami, and T. Shirai, New J. Phys. **8**, 288 (2006).

[22] H. Okamoto and J. Wei, Phys. Rev. E **58**, 3817 (1998).

[23] K. Okabe and H. Okamoto, Jpn. J. Appl. Phys. **42**, 4584 (2003).

[24] A. Piwinski, in *Proc. 9th Int. Conf. on High Energy Accelerators*, Stanford, CA, 1974, p.405 (SLAC, Stanford, 1974).

[25] J. Bjorken and S. Mtingwa, Part. Accel. **13**, 115 (1983).

[26] F. Diedrich et al., Phys. Rev. Lett. **59**, 2931 (1987).

[27] D. J. Wineland et al., Phys. Rev. Lett. **59**, 2935 (1987).

[28] M. Drewsen, C. Brodersen, L. Hornekær, and J. S. Hangst, Phys. Rev. Lett. **81**, 2878 (1998).

[29] H.-J. Miesner et al., Phys. Rev. Lett. **77**, 623 (1996).

[30] N. Madsen et al., Phys. Rev. Lett. **83**, 4301 (1999).

[31] T. Schätz, U. Schramm, and D. Habs, Nature (London) **412**, 717 (2001).

[32] U. Schramm, M. Bussmann, and D. Habs, Nucl. Instrum. Meth. A **532**, 348 (2004).

[33] It is quite easy for any Paul traps to fulfill both conditions (1) and (2). More importantly, the low-energy Coulomb crystals in the circular trap are not exposed to strong momentum dispersion that causes a serious trouble in a real storage ring.

[34] P. P. Ewald, Ann. Phys. (Leipzig) **64**, 253 (1921).

[35] J. Wei, Proc. of PAC'01, Chicago, June 2001, TPPH011, p. 1678 (2001).

[36] H. Okamoto, Phys. Plasmas **9**, 322 (2002).

[37] I. Lauer et al., Phys. Rev. Lett. **81**, 2052 (1998).

[38] M. Ikegami, H. Sugimoto, and H. Okamoto, J. Phys. Soc. Jpn. **77**, 074502 (2008).